Unlocking the Hydrolytic Mechanism of GH92 α-1,2-Mannosidases: Computation Inspires the use of C-Glycosides as Michaelis Complex Mimics

Unlocking the Hydrolytic Mechanism of GH92 α-1,2-Mannosidases: Computation Inspires the use of C-Glycosides as Michaelis Complex Mimics

Santiago Alonso-Gil,*[a] Kamil Parkan,[c] Jakub Kaminský,[d] Radek Pohl,[d] and Takatsugu Miyazaki*[b]

Abstract: The conformational changes in a sugar moiety along the hydrolytic pathway are key to understand the mechanism of glycoside hydrolases (GHs) and to design new inhibitors. The two predominant itineraries for mannosidases go via $^OS_2 \rightarrow B_{2,5} \rightarrow {}^1S_5$ and $^3S_1 \rightarrow {}^3H_4 \rightarrow {}^1C_4$. For the CAZy family 92, the conformational itinerary was unknown. Published complexes of *Bacteroides thetaiotaomicron* GH92 catalyst with a *S*-glycoside and mannoimidazole indicate a $^4C_1 \rightarrow {}^4H_5/$ $^1S_5 \rightarrow {}^1S_5$ mechanism. However, as observed with the GH125 family, *S*-glycosides may not act always as good mimics of GH's natural substrate. Here we present a cooperative study between computations and experiments where our results predict the $E_5 \rightarrow B_{2,5}/{}^1S_5 \rightarrow {}^1S_5$ pathway for GH92 enzymes. Furthermore, we demonstrate the Michaelis complex mimicry of a new kind of *C*-disaccharides, whose biochemical applicability was still a chimera.

Introduction

The regulation of N-glycan modifications is crucial to maintain protein quality control and the functional development of glycoproteins in the endoplasmic reticulum and the Golgi apparatus.[1] Glycoside hydrolases (GHs) are biocatalysts dedicated to cleave glycosidic bonds connecting individual monosaccharides. Several families of GHs are also involved in N-glycan biosynthesis. Some of these enzymes that are involved in the protein folding and the function regulation are essential for the control of congenital disorders of glycosylation – also known as carbohydrate-deficient glycoprotein syndromes.[2,3] Among those catalysts, α-mannosidases are irreplaceable in the regulation of the mannose-containing N-glycan processing. Following the CAZy classification,[4] GH families 38,[5] 47,[6] 76,[7] 92,[8] 99[9] and 125[10] are responsible for N-glycan cleavage.

The inhibition of a GH relates to its enzymatic mechanism. Once the substrate (a saccharide) joins the active site of the hydrolase, the sugar in the −1 subsite (−1 sugar)[11] undergoes a conformational change during hydrolysis. When the process overcomes the highest energy state, also known as the transition state (TS), the −1 sugar becomes an oxocarbenium ion-like moiety.[12] One of the strategies to inhibit a GH is based on designing TS mimics whose conformation is similar to the oxocarbenium ion-like ring.[13–16]

In parallel, developing chemical derivatives of the natural substrate of GHs has emerged as a procedure to inhibit glycosidases. The most common technique utilizes sulfuration of the glycosidic bond (*S*-glycoside).[17] In some experiments, the crystallization of GHs in complex with *S*-glycosides shed light on the conformation of the natural substrate in the Michaelis complex (MC, reactant).[18,19] However, their MC mimicry was not observed in GH125. The natural substrate-related *S*-glycoside predicted a non-distorted −1 sugar moiety, while computations and further experiments showed a distorted one.[20] Comparing the available GH125 complexes reveals (*S*-glycoside – PDB 3QT9,[10] and natural substrate – PDB 5M7I[19]) that the substitution of the glycosidic oxygen by sulfur leads to a lengthening of the glycosidic bond (from 1.45 Å to 1.87 Å) and a C–X–C angular readjustment (from 108.4° to 103.7°). Due to the topology of the GH125 active site, this structural change resulted in a hydrogen bond rearrangement between the −1 sugar and the enzyme, and a consequent conformational change.

[a] Dr. S. Alonso-Gil
     Department of Structural and Computational Biology
     Max F. Perutz Laboratories
     University of Vienna
     Dr.-Bohr-Gasse 9, 1030 Vienna (Austria)
     E-mail: santiago.alonso.gil@univie.ac.at

[b] Dr. T. Miyazaki
     Research Institute of Green Science and Technology
     Shizuoka University
     836 Ohya, Suruga-ku, Shizuoka, 422-8529 (Japan)
     E-mail: miyazaki.takatsugu@shizuoka.ac.jp

[c] Dr. K. Parkan
     Department of Chemistry of Natural Compounds
     University of Chemistry and Technology
     Technická 5, 166 28, Prague (Czech Republic)

[d] Dr. J. Kaminský, Dr. R. Pohl
     Institute of Organic Chemistry and Biochemistry of the Czech Academy of Sciences, Gilead Sciences & IOCB Research Centre
     Czech Academy of Sciences
     Flemingovo nám. 2, 166 10, Prague (Czech Republic)

Chem. Eur. J. **2022**, e202200148 (1 of 6)

© 2022 The Authors. Chemistry - A European Journal published by Wiley-VCH GmbH

Chemistry–A European Journal

Research Article
doi.org/10.1002/chem.202200148

Chemistry Europe
European Chemical
Societies Publishing

Since we talk about the ring mimicry, the conformational study of 6-membered rings (6-rings) is the base to classify and quantify the enzymatic itineraries of GHs. In 1975, Cremer and Pople developed a mathematical expression based on puckering coordinate(s) allowing the graphical representation of the conformational space of a ring.[21] As depicted in Figure 1, a Mercator representation projects the puckering space in a two-dimensional surface where all the conformations of a pyranose ring are presented. In this work, we will use the IUPAC notation of pyranose conformations.[22] By the principle of least nuclear motion,[23] the conformations of the reactants (MC) and products (PC) must surround the TS, following an ideal linear pathway. In α-mannosidases, we observe two main itineraries: $^OS_2 \rightarrow B_{2,5} \rightarrow {}^1S_5$ (GH38, 76, and 125; the expected pathway for GH92, Figure 1 – yellow arrow) and $^3S_1 \rightarrow {}^3H_4 \rightarrow {}^1C_4$ (GH47; the alternative pathway, Figure 1 – blue arrow). Due to the significant double-bond character between the pyranic oxygen and the anomeric carbon, the C2-C1-O5-C5 torsion angle tends to zero, and the conformational space of the TS mimics was recently found around a linear region separating the Mercator surface (Figure 1 – blue line).[15]

In the present work we focus on the inverting Ca^{2+}-dependent *exo*-α-1,2-mannosidase, whose catalytic residues are a proton donor (Glu) and an assistant base (Asp). In Ref. [8], Zhu et al. characterized and crystallized *Bacteroides thetaiotaomicron* GH92 (BT3990, BtGH92) complex with α-1,2-*S*-mannobiose **2** (Figure 2) in the presence and in the absence of Ca^{2+} (MC mimic), and mannoimidazole **4** (Figure 2 – MVL) in the presence of Ca^{2+} (TS mimic). The MC mimic shows an undistorted −1 sugar moiety ($^4C_1$), both in the presence and in the absence of Ca^{2+}. The TS mimic shows a $^4H_5/^1S_5$ distorted conformation. Connecting both regions (Figure 1, green arrow), the experiments show an unexpected $^4C_1 \rightarrow {}^4H_5/^1S_5 \rightarrow {}^1S_5$ pathway. Furthermore, analyzing the available MC mimic complexes (PDB 2WW1 and 2WW3), the catalytic water is not kept in a position allowing the nucleophilic attack (>4 Å), while the TS mimic (PDB 2WZS) shows a water molecule at a distance of ∼3 Å from the anomeric center (Figure 3). This fact and the resulting pathway disrespecting the least nuclear motion principle indicate a possible conformational mismatch between the *S*-glycoside **3** and the natural substrate **1** (as observed in GH125).

While the hydrolytic mechanism of GH92 enzymes remains locked, our goal is to decipher the conformational changes
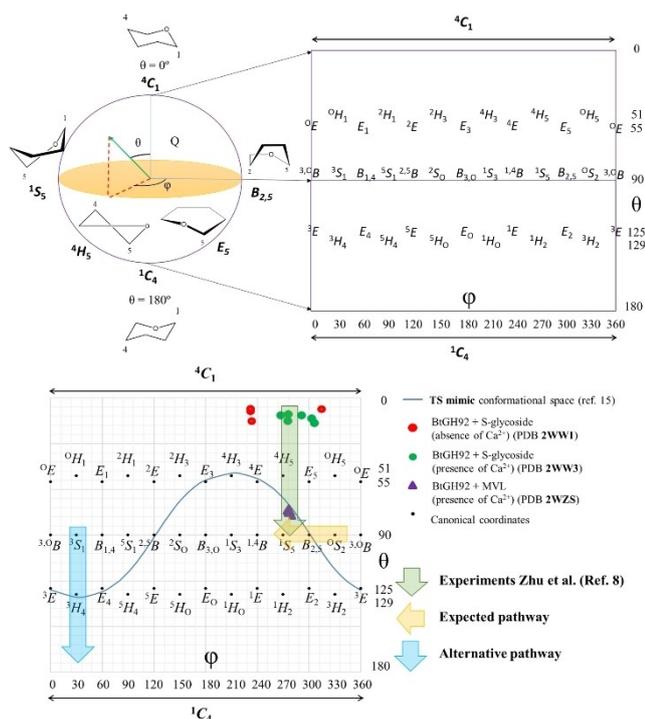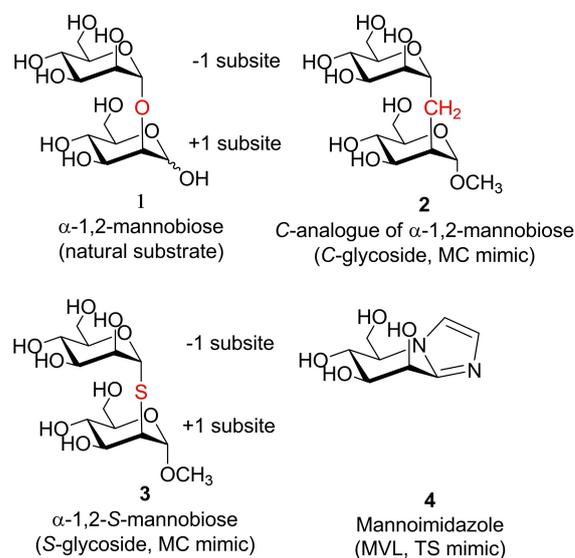

Figure 1. (top) Representation of different conformers of a 6-membered ring molecule (chair – C, boat – B, envelope – E and, half-chair – H, following the IUPAC notation[22]). Mercator projection of the Cremer and Pople's puckering coordinates' sphere for a 6-membered ring. (bottom) −1 sugar moieties in PDB 2WW1 (red dots), 2WW3 (green dots) and 2WZS (purple triangles) are depicted over the Mercator conformational surface. The experiments in Ref. [8] describe the $^4C_1 \rightarrow {}^4H_5/^1S_5 \rightarrow {}^1S_5$ conformational itinerary (green arrow), while the expected (yellow arrow) and alternative (blue arrow) pathways are $^OS_2 \rightarrow B_{2,5} \rightarrow {}^1S_5$ and $^3S_1 \rightarrow {}^3H_4 \rightarrow {}^1C_4$, respectively. The blue line represents an analytical function from Ref. [15] connected to the TS mimic conformational space.

Figure 2. Schematic representation of the molecular structures of the substrates used to study the hydrolytic mechanism of GH92 α-mannosidases (each ring moiety occupies either the −1 or the +1 subsite as noted in this representation).
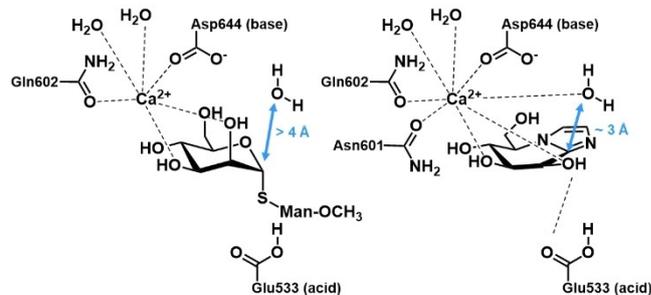

Figure 3. Schematic diagrams of BT3990 (BtGH92) complexed with α-1,2-*S*-mannobiose **3** and mannoimidazole **4**.[8]

Chemistry–A European Journal

Research Article
doi.org/10.1002/chem.202200148

**Chemistry
Europe**
European Chemical
Societies Publishing

occurring over the −1 sugar from the formation of the Michaelis complex to the delivery of the inverted product. Our most burning question in this work solved the structural differences between the *S*-glycoside **3** and MVL **4** complexes (Figure 3), and why is the catalytic water not kept close to the *S*-glycoside. The answer could be related to the abrupt conformational change of the −1 sugar. After the inspection of the structure, we observed the most relevant difference in the vicinity of the Ca^{2+} cation. In the presence of MVL **4**, the catalytic water is coordinated to the calcium cation. In the presence of *S*-glycoside **3**, the hydroxyl group (OH) in carbon 2 (C2) is occupying the position of the catalytic water. With MVL **4**, the hydroxyl at C2 interacts with the proton donor (E533).

Considering all aforementioned evidence, quantum-mechanics (QM) calculations could shed light on the conformational itinerary followed by the natural substrate in GH92 enzymes. Starting from the BtGH92-MVL crystal structure (PDB 2WZS), we constructed a full-QM cluster model of the active site by manual exchange of the MVL moiety for the natural substrate (α-1,2-mannobiose **1**). Keeping the Ca^{2+}-glycoside coordination and hydrogen bond interactions observed in the presence of MVL, we observed a significant conformational change after the geometry optimization. After obtaining computational results, the disagreement between our QM model and the BtGH92 – *S*-glycoside complex required further experimental demonstration.

Since no experimental evidence of the ring distortion existed, our calculation would have appeared just as a theoretical hypothesis. However, two recent works in organic chemistry and biochemistry inspired a strategy to demonstrate distortion of α-1,2-mannobiose **1** when forming a Michaelis complex with GH92 enzymes.[24–26]

On the one hand, the synthesis and conformational analysis of *C*-oligosaccharides[23,24] provided an evidence of a group of molecules capable to mimic natural carbohydrates. On the other hand, Li et al. were capable to characterize and crystallize a Ca^{2+}-dependent α-1,2-mannosidase from *Enterococcus faecalis* (EfGH92), which has two domains like other GH92 mannosidases.[26] Structural superposition between BtGH92 and EfGH92 is provided in the Supporting Information.

C-analogue of α-1,2-mannobiose **2** (Figure 2, compound **2**) was received via previously published procedure using Ni-catalyzed Suzuki-Miyaura cross-coupling reaction followed by stereoselective transformations of obtained *C*-pseudodisaccharide.[27] Furthermore, we performed the cloning and expression of the wild-type (WT) and an acid catalyst mutant (E494Q) of EfGH92 (see Supporting Information for details). Once obtained the different catalysts, we crystalized EfGH92 (WT) with *C*-disaccharide **2** and E494Q (mutant) with the natural α-1,2-mannobiose **1**, and determined their crystal structures at high resolutions. Further synthetic details, conformational analysis of *C*-disaccharide **2** in water solution, and results of the experiments are presented in the Supporting Information.

Furthermore, in order to strengthen the reliability of our calculations, we employed a scan calculation to decipher the conformational itinerary followed by the −1 sugar in the cluster model. In terms of reactivity, the reported kinetic experiments with BtGH92 and α-1,2-mannobiose **1** show a k_{cat} of 87 s^{-1}.[8] Applying the transition state theory,[28] the activation barrier is equivalent to 14.9 kcal·mol^{-1}, reference value for direct comparison with our computational energy barriers.

Results and Discussion

The optimized cluster model (depicted in Figure 4 as MC) presents a distorted $E_5/B_{2,5}$ conformation for the −1 sugar ring. This result differs significantly from the $^4C_1$ conformation observed in the *S*-glycoside **3**. In our scan calculation, the proton in E533 (equivalent to E494 of EfGH92) was transferred to the glycosidic oxygen, the cleavage of the glycosidic bond, and the nucleophilic attack of the catalytic water were activated by constraining the involved distances. The optimized structures of MC, TS ("TS-like") and PC are presented in Figure 4. We obtained the potential energy barriers of $\Delta E^{\neq} = 14.1$ kcal·mol^{-1} and $\Delta E_0 = -2.7$ kcal·mol^{-1}. This result is in good agreement with the available kinetics parameters.[8]

X-ray crystallography showed that WT and the mutant form a tetramer where ligands and Ca^{2+} ions are allocated in each active site cavity (−1 and +1 subsites). On the one hand, three of the four *C*-glycosides **2** attached to WT exist in a conformation corresponding to the QM-optimized cluster model ($E_5/B_{2,5}$), while one outlier presents a $^1S_5/^{1,4}B$ structure (Figure 4 – green dots). On the other hand, the natural substrate **1** attached to the mutant presents one of the four structures in the E_5 region, two of them in the $E_5/^4H_5$ region, and the last one in the $^4H_5/^1S_5$ space (Figure 4 – purple dots). This evidence together with the conformations found in the BtGH92-MVL complex **4** indicate a simplified conformational itinerary crossing the $E_5 \rightarrow {}^1S_5$ region (Figure 4 – green arrow).

Following the −1 sugar conformation along the reaction pathway (Figure 4 – red dots and black dashed line), we can conclude that the itinerary in our cluster model is $E_5/B_{2,5} \rightarrow B_{2,5}/E_5 \rightarrow {}^1S_5/B_{2,5}$. Being aware of the subtle conformational changes observed in the −1 sugar both experimentally and computationally, and the dynamic nature of the biochemical systems, the accuracy of results is limited. The experimental results lead to an MC in the vicinity of E_5 and a TS crossing $^4H_5/^1S_5$. While the calculations suggest an MC in $E_5/B_{2,5}$ and a TS in $B_{2,5}/E_5$. In any case, investigated changes are only minor. Nevertheless, when we slightly simplify the nomenclature, we can conclude that GH92 α-1,2-mannosidase follows an $E_5 \rightarrow B_{2,5}/^1S_5 \rightarrow {}^1S_5$ conformational itinerary (Figure 4, middle).

The analysis of crystal structures of active sites revealed (Figure 5) that the distorted α-D-mannopyranosyl moiety occupies the −1 subsite, while the +1 subsite is occupied by an undistorted 2-CH$_2$- and 2-*O*-mannosyl leaving group. Comparing the EfGH92-*C*-glycoside complex and the PDB 2WW3 (thioglycoside) structure, we observe that the hydroxyl group at C2 of the *S*-glycoside occupies the same position as the catalytic water in the *C*-disaccharide complex. Due to the hydrophobic nature of the pseudo-glycosidic methylene group, the E494 catalytic acid residue changes its orientation, and a
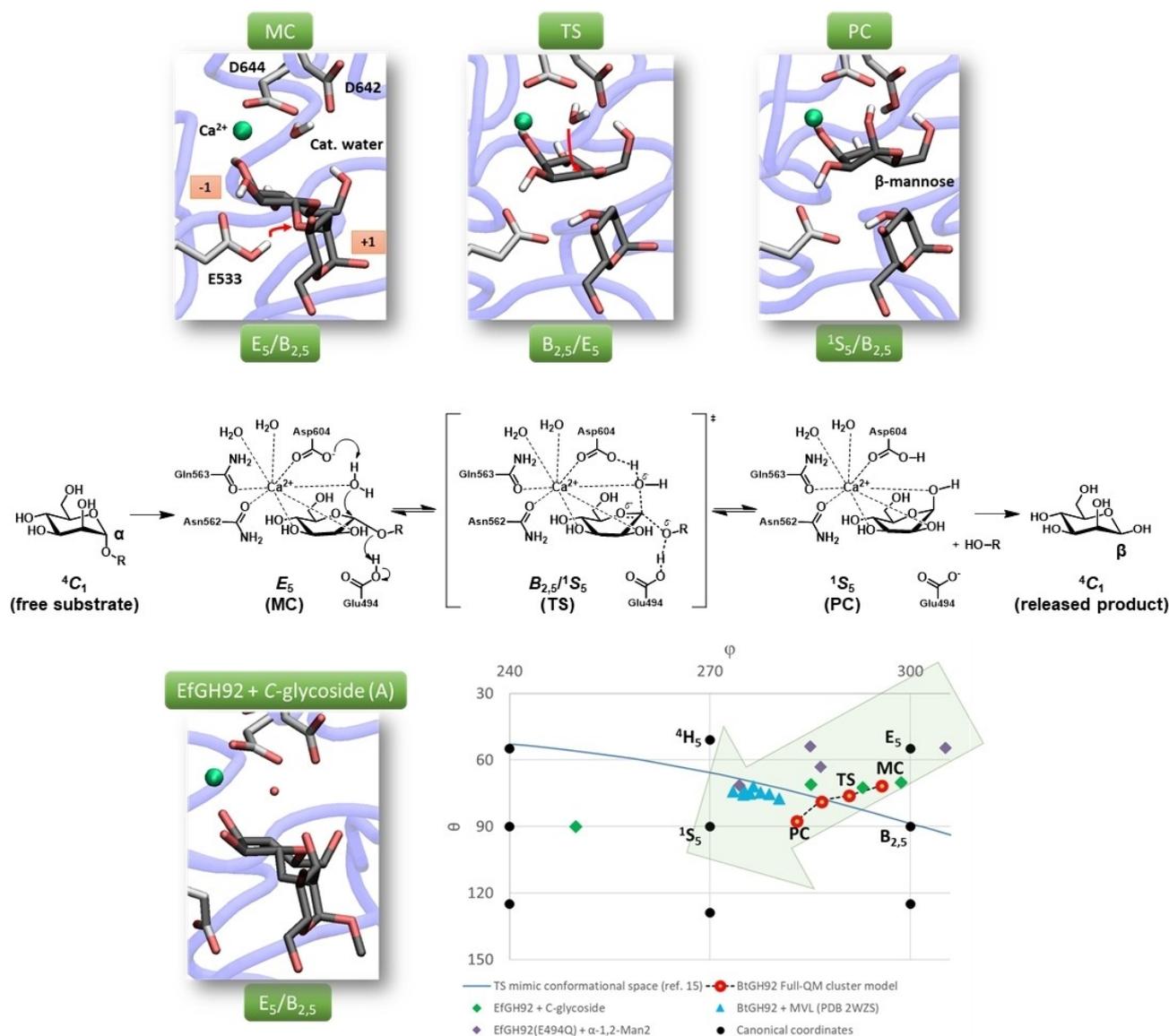
Figure 4. (top) Simplified representative structures of MC, TS and PC of the QM-optimized cluster model of BtGH92 with **1**, (middle) the proposed mechanism for GH92 enzymes and (bottom) the chain A of the EfGH92 enzyme in complex with the *C*-disaccharide **2** (MC mimic), and a zoom view of the puckering coordinates space of the observed −1 sugar moieties in the available experiments and calculations (further details in the Supporting Information).

water molecule interacts with the OH group at C2 of the *C*-glycoside. The closest water to the anomeric carbon is further than 4 Å in case of the *S*-glycoside, while a well-oriented catalytic water is coordinated to Ca^{2+} at ~3 Å from the anomeric center of the *C*-glycoside (Figure 5 – C).

In Figure 5 – D, we also depict the main hydrogen bond interactions present in the E494Q EfGH92-mannobiose complex. As observed in the QM-optimized BtGH92 cluster model, the OH group at C2 interacts with the oxygen of the mutated glutamine residue Q494. The NH_2 group of the mutated residue interacts with the glycosidic oxygen, properly oriented for a hypothetic proton transfer. The hydroxyls at C3 and C4 interact with aspartic acid D313. The catalytic water interacts with two aspartic acid residues, D602 and D604. Finally, the hydroxymethyl arm interacts with a water molecule and serine

S66. These observations are in good agreement with the interactions observed in our calculations, strengthening the viability of the model.

Conclusion

In conclusion, computations in this study have newly been a powerful tool to decrypt the reaction mechanism of an enzyme-substrate biosystem. Both experimental results and calculations confirm that the catalytic mechanism of GH92 α-1,2-mannosi-dases follows the $E_5 \rightarrow B_{2,5}/^1S_5 \rightarrow {}^1S_5$ itinerary (Figure 4). As observed in GH125 enzymes, *S*-glycosides may not act as good MC mimics, due to different interaction patterns with the active site residues, and, in this case, also, with a metal cation. The
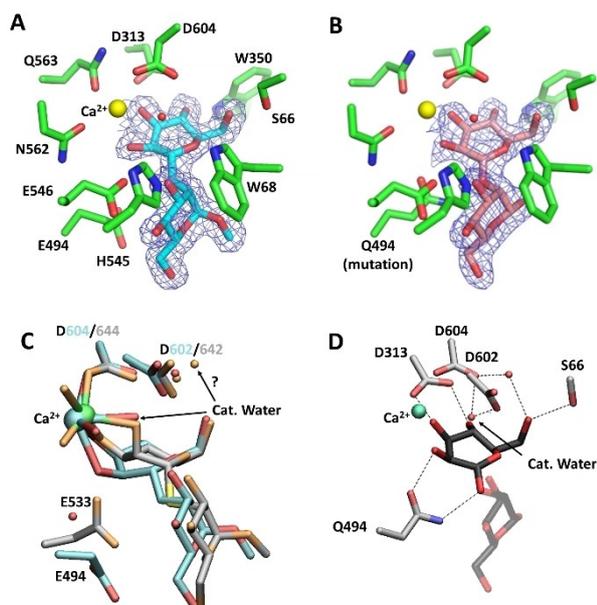
Chem. Eur. J. **2022**, e202200148 (4 of 6)

© 2022 The Authors. Chemistry - A European Journal published by Wiley-VCH GmbH

Chemistry–A European Journal

Research Article
doi.org/10.1002/chem.202200148

Chemistry Europe
European Chemical
Societies Publishing

Figure 5. Active sites and observed electron densities ($2F_o$-F_c, 1σ) of (A) WT EfGH92 in complex with *C*-disaccharide **2**, and (B) E494Q EfGH92 in complex with α-1,2-mannobiose. (C) Structural superposition of the active sites of BtGH92 in complex with α-1,2-*S*-mannobiose **3** (PDB 2WW3, grey and orange), and EfGH92 in complex with **2** (this work, cyan and red). The OH in C2 of the *S*-glycoside occupies the same position as the catalytic water in presence of the *C*-disaccharide. (D) Main hydrogen bond interactions observed in the active site of E494Q EfGH92 in complex with α-1,2-mannobiose. The OH in C2 interacts with the free oxygen of the mutated catalytic acid Q494 residue.

conformational difference between the *C*-glycoside and the *S*-glycoside allows the approach of the catalytic water to the anomeric carbon, in the first case, where the water is coordinated with the Ca^{2+} cation. We identify a new class of MC mimic through the substitution of glycosidic oxygen by the CH_2 group. This chemical change keeps the conformation of the sugar, but the glycosidic position becomes hydrophobic, suppressing thus the interaction with the catalytic residue.

Experimental Section

Protein production and crystallography procedures, details about the synthesis and conformational study of the *C*-analogue of α-1,2-mannobiose **2** and computational details are available in the Supplementing Information.

Structural data availability

The atomic coordinates and structure factors have been deposited in the Worldwide Protein Data Bank (http://wwpdb.org/) under accession codes 7FE1 and 7FE2.

Conflict of Interest

The authors declare no conflict of interest.

Data Availability Statement

The data that support the findings of this study are available in the supplementary material of this article.

[1] L. W. Ruddock, M. Molinari, *J. Cell Sci.* **2006**, *119*, 4373–4380.
[2] G. Z. Lederkremer, *Curr. Opin. Struct. Biol.* **2009**, *19*, 515.
[3] H. H. Freeze, H. Schachter. Genetic Disorders of Glycosylation. In: A. Varki, R. D. Cummings, J. D. Esko, editors. *Essentials of Glycobiology. 2nd edition*, Cold Spring Harbor (NY): Cold Spring Harbor Laboratory Press, **2009**. Chapter 42.
[4] V. Lombard, H. Golaconda Ramulu, E. Drula, P. M. Coutinho, B. Henrissat, *Nucleic Acids Res.* **2014**, *42*, D490–5.
[5] B. Cobucci-Ponzano, F. Conte, A. Strazzulli, C. Capasso, I. Fiume, G. Pocsfalvi, M. Rossi, M. Moracci, *Biochimie* **2010**, *92*, 1895–1907.
[6] S. W. Mast, K. W. Moremen, *Meth. Enzymol.* **2006**, *415*, 31–46.
[7] J. Roth, M. Ziak, C. Zuber, *Biochimie* **2003**, *85*, 287–294.
[8] Y. Zhu, M. D. L. Suits, A. J. Thompson, S. Chavan, Z. Dinev, C. Dumon, N. Smith, K. W. Moremen, Y. Xiang, A. Siriwardena, S. J. Williams, H. J. Gilbert, G. J. Davies, *Nat. Chem. Biol.* **2009**, *6*, 125–132.
[9] A. J. Thompson, R. J. Williams, Z. Hakki, D. S. Alonzi, T. Wennekes, T. M. Gloster, K. Songsrirote, J. E. Thomas-Oates, T. M. Wrodnigg, J. Spreitz, A. E. Stütz, T. D. Butters, S. J. Williams, G. J. Davies, *Proc. Nat. Acad. Sci.* **2012**, *109*, 781–786.
[10] K. J. Gregg, W. F. Zandberg, J–H. Hehemann, G. E. Whitworth, L. Deng, D. J. Vocadlo, A. B. Boraston, *J. Biol. Chem.* **2011**, *286*, 15586–15596.
[11] G. J. Davies, K. S. Wilson, B. Henrissat, *Biochem. J.* **1997**, *321*, 557–669.
[12] J. D. McCarter, S. Withers, *Curr. Op. Struc. Biol.* **1994**, *4*, 885–892.
[13] T. M. Gloster, G. J. Davies, *Org. Biomol. Chem.* **2010**, *8*, 305–320.
[14] C. Colombo, A. J. Bennet, *Adv. Phys. Org. Chem.* **2017**, *51*, 99–127.
[15] S. Alonso-Gil, *J. Carbohydr. Chem.* **2020**, *39*, 175–188.
[16] W. Ren, M. Farren-Dai, N. Sannikova, K. Swiderek, Y. Wang, O. Akintola, R. Britton, V. Moliner, A. J. Bennet, *Chem. Sci.* **2020**, *11*, 10488–10495.

[17] M. Qiao, L. Zhang, R. Jiao, S. Zhang, B. Li, X. Zhang, *Tetrahedron* **2021**, *81*, 131920.

[18] A. J. Thompson, G. Speciale, J. Iglesias-Fernandez, Z. Hakki, T. Belz, A. Cartmell, R. J. Spears, E. Chandler, M. J. Temple, J. Stepper, H. J. Gilbert, C. Rovira, G. J. Davies, *Angew. Chem. Int. Ed.* **2015**, *54*, 5378–5382.

[19] J. Zou, G. J. Kleywegt, J. Stahlbert, H. Driguez, W. Nerinckx, M. Claeyssens, A. Koivula, T. T. Teeri, T. A. Jones, *Structure* **1999**, *7*, 1035–1045.

[20] S. Alonso-Gil, A. Males, P. Z. Fernandes, S. J. Williams, G. J. Davies, C. Rovira, *J. Am. Chem. Soc.* **2017**, *139*, 1085–1088.

[21] D. Cremer, J. A. Pople, *J. Am. Chem. Soc.* **1975**, *97*, 1354–1358.

[22] A. Bérces, D. M. Whitfield, T. Nukada, *Tetrahedron* **2001**, *57*, 477–491.

[23] M. L. Sinnott, *Adv. Phys. Org. Chem.* **1988**, *24*, 113.

[24] B. Bertolotti, B. Oroszova, I. Sutkeviciute, L. Kniezo, F. Fieschi, K. Parkan, Z. Lovyova, M. Kasakova, *Carbohydr. Res.* **2016**, *435*, 7–18.

[25] I. Raich, Z. Lovyová, L. Trnka, K. Parkan, J. Kessler, R. Pohl, J. Kaminský, *Carbohydr. Res.* **2017**, *451*, 42–50.

[26] Y. Li, R. Li, H. Yu, X. Sheng, J. Wang, A. J. Fisher, X. Chen, *FEBS Lett.* **2020**, *594*, 439–451.

[27] B. Oroszová, J. Choutka, J. R. Pohl, K. Parkan, *Chem. Eur. J.* **2015**, *21*, 7043–7047.

[28] D. G. Truhlar, B. C. Garrett, S. J. Klippenstein, *J. Phys. Chem.* **1996**, *100*, 12771–12800.

RESEARCH ARTICLE

Glycoside hydrolase 92 enzymes catalyze the degradation of N-glycans containing chains of α-mannose. Since experiments with *S*-glycosides did not shed light about the conformation of the Michaelis complex (MC), we present a multidisciplinary work where computation and experiments demonstrate the reactive conformation adopted by the sugar in the MC. In addition, we demonstrate the power of *C*-glycosides as MC mimics.

Dr. S. Alonso-Gil*, Dr. K. Parkan, Dr. J. Kaminský, Dr. R. Pohl, Dr. T. Miyazaki*

1 – 7

Unlocking the Hydrolytic Mechanism of GH92 α-1,2-Mannosidases: Computation Inspires the use of C-Glycosides as Michaelis Complex Mimics